Desalination and Water Treatment
www.deswater.com
doi: 10.1080/19443994.2013.876672

54 (2015) 166–177
April

Taylor & Francis
Taylor & Francis Group

Comparative studies on the olive stone activated carbon adsorption of Zn^{2+}, Ni^{2+}, and Cd^{2+} from synthetic wastewater

Tamer M. Alslaibi[a], Ismail Abustan[a,*], Mohd Azmier Ahmad[b], Ahmad Abu Foul[c]

[a]*School of Civil Engineering, Universiti Sains Malaysia, Engineering Campus, Nibong Tebal, Pulau Pinang 14300, Malaysia Tel. +60 4 5996259; Fax: +60 4 5941009; email: ceismail@eng.usm.my*
[b]*School of Chemical Engineering, Universiti Sains Malaysia, Engineering Campus, Nibong Tebal, Pulau Pinang 14300, Malaysia*
[c]*Environmental Engineering, Islamic University of Gaza, Gaza, Palestine*

Received 29 July 2013; Accepted 13 December 2013

ABSTRACT

The adsorption of a group of heavy metals namely, Zn^{2+}, Ni^{2+}, and Cd^{2+} onto olive stones activated carbon (OSAC) was carried out in this work. The effects of different reaction parameters, such as the adsorbent dosage, contact time, shaking speed, and initial pH, on pollutant removal efficiency were investigated. Adsorption of Zn^{2+}, Ni^{2+}, and Cd^{2+} was effectively explained by Langmuir and Freundlich isotherms. OSAC efficiently removed 99.03% Zn^{2+}, 97.34% Ni^{2+}, and 94.88% Cd^{2+} at pH 5 and shaking speed 200 rpm. Surface characteristics of the prepared AC were examined by pore structure analysis, scanning electron microscopy, and Fourier transform infrared spectroscopy. The Brunauer-Emmett-Teller surface area, total pore volume and average pore diameter of the prepared AC were 886.72 m^2/g, 0.507 cm/g, and 4.22 nm, respectively. The equilibrium data of the adsorption were fitted well to the Langmuir and the highest value of adsorption capacity (Q) on the OSAC was found for Zn^{2+} 11.14 mg/g, followed by Ni^{2+} 8.42 mg/g and Cd^{2+} 7.80 mg/g. A pseudo-second-order model sufficiently described the adsorption kinetics, which indicated that the adsorption process was controlled by chemisorption. The results revealed that the OSAC has the potential to be used as a low-cost adsorbent for the treatment of wastewaters contaminated with heavy metals.

Keywords: Olive stone; Activated carbon; Adsorption; Isotherm; Heavy metals; Kinetics

1. Introduction

The removal of toxic metals from wastewater is a matter of great interest in the field of water pollution, which is a serious cause of environmental degradation. Heavy metals, such as Cu^{2+}, Cd^{2+}, Ni^{2+}, Pb^{2+}, Fe^{2+}, and Zn^{2+} are toxic to human beings and other living organisms when their concentrations exceed the acceptance limit. These heavy metals appear in wastewater discharged from hospitals [1] and different industries, including smelting, metal plating, Cd–Ni battery and alloy manufacturing, as well as phosphate fertilizer, mining pigment, and stabilizer production [2–5]. Although the commercially available activated carbon (AC) has been reported to be a suitable sorbent material, its high cost resulting from the use of non-renewable and relatively high-cost starting material such as coal makes this sorbent not

*Corresponding author.

competitive from the economical point of view [6]. Then, it would be very interesting to find out an application to reuse other precursors of AC production especially from agricultural wastes which are inexpensive, abundantly available and renewable materials [7]. From the literature, tobacco stems [8], rice husks [9], almond shells [10], citrus reticulate [11], corn cobs [12], coriolus versicolor [13], waste apricot [14], sawdust [15], date palm leaflets [16], rose waste [17], rosa gruss an teplitz [18], mentha arvensis [19], and cherry stones [20] were used to prepare ACs.

According to the international olive council, the annual production of olive oil in the world in the year 2012 is more than 3 million tons, translating to approximately 15 million tons of olive cakes as the by-products [21]. Olive stone waste residue as a raw material for the production of AC can be considered as one of the best candidate among the agricultural wastes because it is cheap and quite abundant, especially in Mediterranean countries [22,23].

However, the use of AC prepared from olive stones by chemical activation with KOH for heavy metals removal is not well established. So, the aim of this study is to compare and evaluate the effectiveness of the olive stone activated carbon (OSAC) for removing Zn^{2+}, Ni^{2+}, and Cd^{2+} from synthetic wastewater. To investigate the process variables (i.e. dosage, contact time, shaking speed, and initial pH), suitable isotherm models and kinetics coefficients of the OSAC for the removal of Zn^{2+}, Ni^{2+}, and Cd^{2+} are used.

2. Material and methods

2.1. Aqueous solution

Approximately 1,000 mg/L of stock solution was prepared by dissolving appropriate amounts of Zn $(NO_3)_2{\cdot}6H_2O$, $NiCl_2{\cdot}6H_2O$(s), and $CdCl_2{\cdot}H_2O$(s) in deionized water. Then, 20 mg/L test solution of Zn^{2+}, Ni^{2+}, and Cd^{2+} was prepared by successive dilution of the stock solution. Metal standard solution of 1,000 mg/L purchased from Merck was used for inductively coupled plasma optical emission spectroscopy (ICP-Optical Emission Spectrometer; VARIAN 715-ES) calibration.

2.2. Preparation and characterization of AC

OS waste was obtained from Gaza, Palestine. The OS waste was rinsed thrice with hot water, thrice with cold water, and dried in an oven at 105˚C for 24 h to remove moisture content. Once dried, they were ground and sieved for a particle sizes of 2.0–4.75 mm and loaded in a stainless steel vertical tubular reactor placed in a tube furnace [24]. The precursor was mixed with KOH pellets at a ratio of 1:1.25. Deionized water was then added to dissolve all the KOH pellets. Impregnation was performed for 24 h at room temperature, thus incorporating all the chemicals into the core of the particles. After impregnation, the solution was filtered to obtain the residual precursor. The activation step was conducted at 600˚C for 2 h under a nitrogen flow of 150 cm^3/min at a heating rate of 10˚C/min in a muffle furnace for the optimization of the reaction parameters. However, for the isotherm and kinetics examination, parameters such as temperature of 715˚C, activation time of 2 h, and chemical impregnation ratio of 1.53 were maintained [23]. The sample was then cooled to room temperature under nitrogen flow and washed with hot deionized water and 0.1 M HCl until the pH of the washed solution was within the range 6.5–7.

2.3. BET and SEM of the prepared AC

The surface area, pore volume, and average pore diameter of the OSAC were determined by using Micromeritics ASAP 2020 volumetric adsorption analyzer. The Brunauer-Emmett-Teller (BET) surface area was measured from the adsorption isotherm using BET equation. The total pore volume was estimated to be the liquid volume of nitrogen at a relative pressure of 0.98. The surface morphology of the samples was examined using a scanning electron microscope (Quanta 450 FEG, the Netherlands). The proximate analysis was carried out using a thermogravimetric analyser (Perkin Elmer TGA7, USA).

2.4. Batch equilibrium studies

Batch equilibrium tests were carried out for adsorption of Zn^{2+}, Ni^{2+}, and Cd^{2+} on the OSAC. The effects of adsorbent dosage, contact time, shaking speed, and initial pH on the adsorption uptake were investigated. Optimization of the media performance was achieved by monitoring the influence of one factor at a time on an experimental response. This optimization is called the one-variable-at-a-time method. Whereas only one variable is varied, others are maintained at a constant level [25].

All batch adsorption experiments were performed by shaking 100 mL of synthetic solution of these heavy metals in 250 mL volumetric flask using an orbital shaker (Lab. Companion, Model SK-600). Different dosages of OSAC, with particle sizes in the range 2–4.75 mm, were added to each flask and kept in an isothermal shaker for different shaking speeds at 30˚C until equilibrium was reached. After agitation, the solid was removed by filtration through a 0.45 μm

pore size Whatman membrane filter paper. The final metal concentrations in the filtrates as well as in the initial solution were determined by inductively coupled plasma optical emission spectroscopy (ICP; VARIAN 715-ES) calibration. The sorbed metal concentrations were obtained from the difference between initial and final metal concentrations in solution. The amount of adsorption at equilibrium, q_e (mg/g), was calculated using Eq. (1):

$$q_e = \frac{(C_0 - C_e)V}{W} \quad (1)$$

where C_0 and C_e (mg/L) are the liquid-phase concentrations of Zn^{2+}, Ni^{2+}, and Cd^{2+} at initial state and at equilibrium, respectively. V (L) is the volume of solution and W (g) is the mass of dry adsorbent used.

The percentage removal at equilibrium was calculated using Eq. (2):

$$\text{Removal } (\%) = \frac{C_0 - C_e}{C_0} \times 100 \quad (2)$$

where C_0 and C_e are the liquid-phase concentrations at initial state and at equilibrium (mg/L), respectively.

2.4.1. Effect of adsorbent dosage

The adsorbent OSAC dosage is an important parameter for evaluating the quantitative uptake of pollutants. The shaking speed, contact time, and initial pH were 200 rpm, 3 h and 4.5, respectively. The dosages of OSAC adsorbent used were 0, 0.025, 0.05, 0.1, 0.15, 0.2, 0.25, 0.3, 0.4, 0.5, 1.0, and 2.0 g. The control experiments were conducted by repeating all the procedures in the absent of media. Removal percentage was calculated using Eq. (2).

2.4.2. Effect of contact time

The effect of contact time was determined by conducting the experiment at the predetermined OSAC dosage. This was done by shaking ten 250 mL conical flasks containing 100 mL of synthetic solution of heavy metals having a concentration 20 mg/L. The contact times used in the experiment were 0.5, 0.166, 0.333, 0.5, 0.666, 1.0, 2.0, 3.0, 6.0, 18.0, and 24.0 h, with shaking speed of 200 rpm and initial pH of 4.5. Removal percentage was calculated using Eq. (2).

2.4.3. Effect of shaking speed

In order to study the effect of shaking speed, the OSAC dosage and contact time obtained from the previous sections (Sections 2.4.1 and 2.4.2) were used. The pH was 4.5 and the batch experiments were performed at different shaking speed 50, 100, 150, 200, 250, and 300 rpm. Removal percentage was calculated using Eq. (2).

2.4.4. Effect of solution pH

The effect of solution pH on the adsorption process was studied by varying the initial pH of the solutions from 2 to 6 using 0.1 M solution of HCI or NaOH and was measured using a pH meter (WIT-ENG, W-100, Germany). These pH ranges were chosen in order to avoid metal solid hydroxides precipitation. In the case of the metals under study, metal hydroxide precipitation occurs at pH > 7 for $Zn(OH)_2$(s) [26], pH > 8.3 for $Ni(OH)_2$(s) [27] and pH > 9.0 for $Cd(OH)_2$(s) [28]. The experiments were conducted at the predetermined OSAC dosage, contact time, and shaking speed from the previous sections (Sections 2.4.1, 2.4.2, and 2.4.3).

2.5. Batch kinetic studies

The procedure of kinetic adsorption tests was identical to that of batch equilibrium tests; however, the aqueous samples were taken at preset time intervals. The concentrations of Zn^{2+}, Ni^{2+}, and Cd^{2+} were found to be similar. The Zn^{2+}, Ni^{2+}, and Cd^{2+} uptake at any time, q_t (mg/g), was calculated by:

$$q_t = \frac{(C_0 - C_t)V}{W} \quad (3)$$

where C_t (mg/L) is the liquid-phase concentration of Zn^{2+}, Ni^{2+}, and Cd^{2+} at any time, t (h).

3. Results and discussion

3.1. Characterization of OSAC

Among the most important features of adsorbents are their surface area and porosity. The BET surface area, mesopore surface area, total pore volume, and average pore diameter of the prepared AC were 886.72 m^2/g, 740.66 m^2/g, 0.507 cm^3/g, and 4.92 nm, respectively. The average pore diameter of 4.92 nm

indicated that the OSAC was in the mesoporous region [29]. The high surface area and pore volume of the OSAC were due to the activation process used which involved KOH. The proximate values of the precursor and OSAC are presented in Table 1. After the activation process, the volatile matter content decreased significantly, whereas the fixed carbon content increased in OSAC. This resulted from the pyrolytic effect, by which most of the organic substances are degraded and discharged as gas and liquid tars leaving a material with high carbon purity [30].

Fig. 1(a) and (b) shows the scanning electron microscopy (SEM) images of the precursor and the derived AC, respectively. Large and well-developed pores were obviously formed on the surface of the AC compared with the original precursor. KOH and the activation process are effective in forming well-developed pores on the OSAC surfaces, leading to AC with large surface area and good porous structure (mesopores). Almost all heterogeneous types of pore structure were also distributed on the OSAC surface. Several authors have found similar observations in their works of preparing ACs from walnut shells [31], jute and coconut fibers [32] and bamboo waste [33].

Table 1
Proximate analysis

	Proximate analysis (%)			
Sample	Moisture	Volatile	Fixed carbon	Ash
OS raw	8.70	65.31	18.53	7.46
OSAC	4.20	20.35	71.17	4.28

From Fig. 2(a) and (b), the region between 3,861 and 3,587 cm^{-1} is related to the –OH (hydroxyl) functional groups, and the broad band at 2,387–2,098 cm^{-1} is assigned to the –COOH and C≡C derivatives. The sharp peak at 1,531 cm^{-1} is ascribed to the vibration of C=C stretching of aromatic group, and the signal at 590 cm^{-1} is associated with the C≡C stretching of alkyne group and C-H stretching in alkanes group. Other major peaks also detected at bandwidths 1,905, 1,729, and 987 cm^{-1} assigned to C=O stretching of aldehydes and ketones group, and C-H stretching in alkanes group, respectively.

As demonstrated from Fig. 2(a) and (b), the Fourier transform infrared spectroscopy (FT-IR) spectrum of the prepared AC shows some shift and elimination of the peak, indicative of the modification of surface chemistry and destruction of some intra-molecular bonding under the thermal degradation during the carbonization and activation processes.

3.2. Effect of adsorbent dosage

The adsorbent OSAC dosage is an important parameter for analyzing the quantitative uptake of pollutants. The retention of the pollutants was examined in relation to the amount of adsorbent. The results of the removal of Zn^{2+}, Ni^{2+}, and Cd^{2+} using OSAC are shown in Fig. 3. The shaking speed, contact time, and initial pH level were 200 rpm, 3 h, and 4.5, respectively. The dosage of the OSAC adsorbent varied from 0.025 to 2 g. The percentage of pollutant removal increased with increasing dosages of the OSAC then becomes constant. The best results were obtained using a dosage of 0.3 g, where 99.99% Zn,

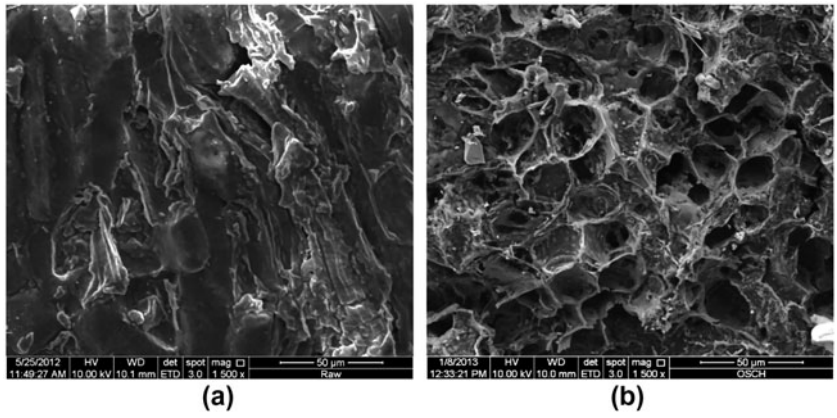

Fig. 1. Scanning electron micrograph: (a) OS raw and (b) OSAC (magnifications: 1500 ×).

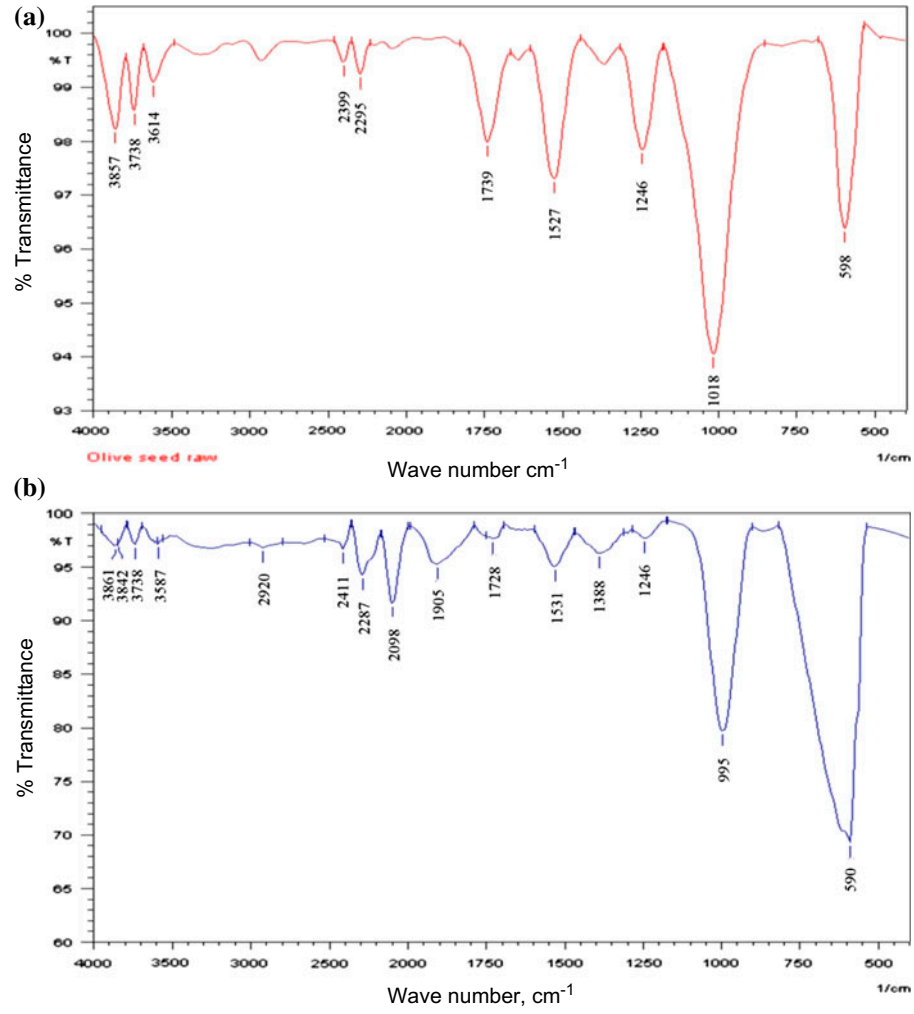

Fig. 2. FTIR spectrums: (a) OS raw and (b) OSAC.

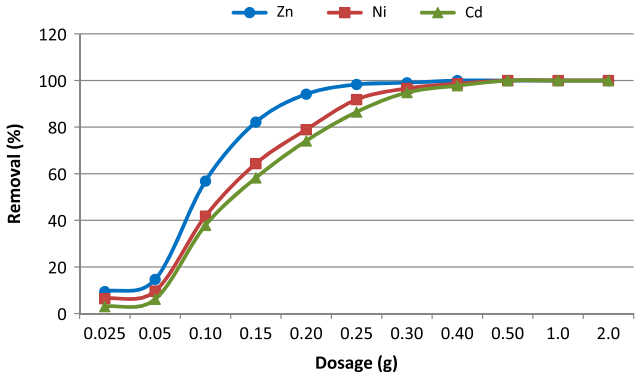

Fig. 3. Effect of OSAC dosages on Zn^{2+}, Ni^{2+}, and Cd^{2+} removal by OSAC.

96.60% Ni, and 94.81% Cd were removed. A greater dosage leads to an increase in Zn^{2+}, Ni^{2+}, and Cd^{2+} which results in significantly lower uptake. This was the reason that the number of available adsorption sites was increased by increasing the adsorbent dose [25,34]. For all the subsequent experiments, an OSAC dosage of 0.3 g was selected.

3.3. Effect of contact time

Fig. 4 shows the effects of contact time on the Zn^{2+}, Ni^{2+}, and Cd^{2+} uptakes. The contact time for the OSAC (dosage of 0.3 g; solution volume of 100 mL; shaking speed of 200 rpm; and initial pH of 4.5) varied from 0.1 to 24 h. It was observed that the Zn^{2+}, Ni^{2+}, and Cd^{2+} adsorption was fast at initial stage of 3 h, thereafter it became slower until it reached a constant value where no more metals can be removed from the solution. The rapid adsorption of metals was due to the fact that at initial stage, a large number of surface sites are available for adsorption. After a lapse of time,

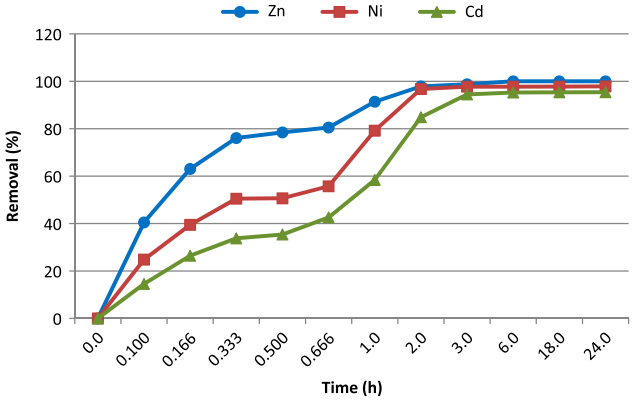

Fig. 4. Effect of contact time on Zn^{2+}, Ni^{2+}, and Cd^{2+} removal by OSAC.

the remaining surface sites are difficult to be occupied due to the repulsion between the solute molecules of the solid and bulk phases [35].

3.4. Effect of shaking speed

The effects of shaking speed on Zn^{2+}, Ni^{2+}, and Cd^{2+} removal are explained in Fig. 5. The effects were studied using 0.3 g of OSAC with a contact time of 3 h and different shaking speeds (50–350 rpm). The results indicated that the removal of the metals increased as the shaking speed increased up to 200 rpm; at higher speeds, the removal rate remained constant. According to Chabani et al. [36], at strong agitation rates the resistance of the boundary layer surrounding the adsorbate weakens.

3.5. Effect of solution pH

The removal of metal ions from aqueous solution by adsorption is highly dependent on the pH of the solution, which affects the surface charge of the adsorbent and the degree of ionization and speciation of the adsorbate [37,38]. To verify the effect of pH on Zn^{2+}, Ni^{2+}, and Cd^{2+} removal using OSAC as adsorbent, experiments were conducted by modifying the pH value from 2 to 6 as shown in Fig. 6. Initially, at low pH < 3, the minimal removal may be due to the higher concentration and high mobility of the H^+, which competes with metal ions on the active sites on sorbents surface and preferentially adsorbed rather than the metal ions [39]. Therefore, H^+ ions react with anionic functional groups on the surface of OSAC and results in the reduction in the number of binding sites available for the adsorption of Zn^{2+}, Ni^{2+}, and Cd^{2+}. In Fig. 5, the percentages of Zn^{2+}, Ni^{2+}, and Cd^{2+} removal were found to increase significantly with increase in solution pH from pH 3 to 6. The highest Zn^{2+}, Ni^{2+}, and Cd^{2+} removal of 99.03%, 97.34%, and 94.88 were achieved at pH 5, respectively. This increase may be due to the presence of negative charge on the surface of the adsorbent that may be responsible for metal binding because solution pH can affect the charge of OSAC surfaces [40]. In addition, at higher pH values, the lower number of H^+ and greater number of ligands with negatives charges result in greater metal adsorption. On other words, monovalent cations, $Me(OH)^+$, are the dominant ion species at the optimal pH range. Based on experimental results and the speciation of metal ions, metal removal by OSAC may have occurred by complexing between the negatively charged functional groups such as carboxylic groups (–COOH) [39,41,42] and metal cations such as Me^{+2} and $Me(OH)^+$. At pH higher than 3–4, carboxylic groups are deprotonated and negatively charged. Accordingly, the attraction of positively charged metal ions would be improved [38]. Thereafter, at pH 5–6, the metal removal remains almost constant. So, for all the subsequent experiments, an initial solution pH of 5 was selected to avoid metal hydroxide precipitation which occurs at pH > 7 for $Zn(OH)_2(s)$ [26], pH > 8.3

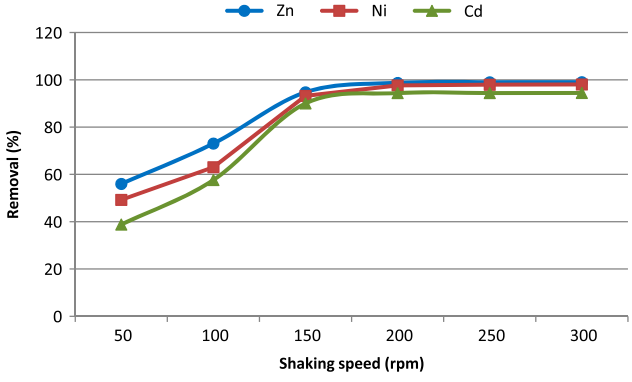

Fig. 5. Effect of shaking speed on Zn^{2+}, Ni^{2+}, and Cd^{2+} removal by OSAC.

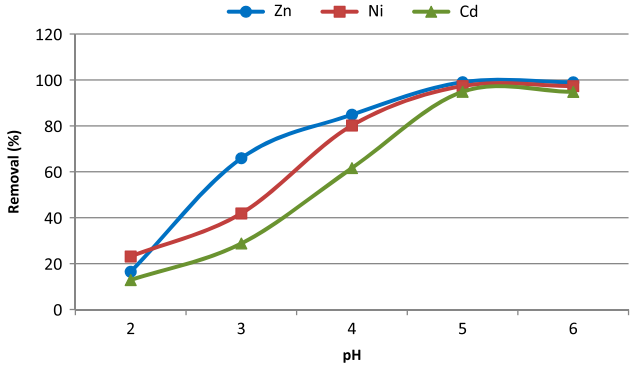

Fig. 6. Effect of solution pH on Zn^{2+}, Ni^{2+}, and Cd^{2+} removal by OSAC.

for $Ni(OH)_2$(s) [27], and pH > 9.0 for $Cd(OH)_2$(s) [28]. The same trend was observed by several researchers that studied metal sorption by different biomaterials, i.e. lead and cadmium by [43], cadmium by orange wastes [42], and zinc, lead, and cadmium by jute fibres [44].

3.6. Adsorption isotherms

Langmuir model is based on the assumption that adsorption energy is constant and independent of surface coverage. The maximum adsorption happens once the surface is covered by a monolayer of adsorbate [45]. The linear form of Langmuir isotherm equation is given as:

$$\frac{1}{(q_e)} = \frac{1}{QbC_e} + \frac{1}{Q} \tag{4}$$

where C_e (mg/L) is the equilibrium liquid-phase concentration of metals; q_e (mg/g) is the equilibrium uptake capacity; Q (mg/g) is the Langmuir constant related to adsorption capacity and b (L/mg) is the Langmuir constant related to energy of sorption which reflects quantitatively the affinity between the sorbent and the sorbate. A straight line was obtained when $1/(q_e)$ was plotted against $1/C_e$. Q was evaluated from the slope, whereas b was determined from the intercept as shown in Fig. 7(a). The equilibrium data were fitted to the Langmuir isotherm. The constants together with the R^2 value are listed in Table 2. As shown in Table 2, the highest value of adsorption capacity (Q) on the OSAC was found for Zn^{2+} 11.14 mg/g, followed by Ni^{2+} 8.42 mg/g and Cd^{2+} 7.80 mg/g. Similarly, the relative affinity order of OSAC, found on the basis of b values, was Zn > Ni > Cd. Therefore, the affinity series found is in agreement with the first hydrolysis constant ($Me(OH)^+$) series, which is: Zn > Ni > Cd [46]. The characteristics of the Langmuir isotherm can be expressed using the equilibrium parameter R_L [47]:

$$R_L = \frac{1}{(1 + bC_0)} \tag{5}$$

where b is the Langmuir constant and C_0 is the initial pollutant concentration (mg/L). The value of R_L indicates whether the isotherm is unfavorable ($R_L > 1$), linear ($R_L = 1$), favorable ($0 < R_L < 1$), or irreversible ($R_L = 0$). The R_L values for adsorption of Zn^{2+}, Ni^{2+}, and Cd^{2+} on the OSAC were 0.007, 0.01, and 0.013, respectively, indicating that the adsorption is a favorable process.

Freundlich model is based on sorption on a heterogeneous surface of varied affinities. The linear form of Freundlich model was given as:

$$\log q_e = \log K + \frac{1}{n}\log C_e \tag{6}$$

where q_e (mg/g) is the amount of metals adsorbed at equilibrium, C_e (mg/L) is adsorbate concentration, K_f $(m/g)(L/mg)^{1/n}$ is the Freundlich constant related to adsorption capacity, and $1/n$ is Freundlich constants related to sorption intensity of the sorbent. Larger values of K_f mean greater capacities of adsorption [48].

The slope of $1/n$, ranging between 0 and 1, is a measure of the adsorption intensity or surface heterogeneity; it becomes more heterogeneous as its value nears 0. A value of $1/n < 1$ indicates a normal Freundlich isotherm, whereas $1/n > 1$ is indicative of cooperative adsorption [49]. The plot of log q_e vs. log C (Fig. 7(b)) gives a straight line with a slope of $1/n$. The value of K was calculated from the intercept value. The values of K, $1/n$, and the linear regression correlation (R^2) for the Freundlich model are given in Table 2.

The results indicate that the adsorption intensities were derived from the Freundlich coefficient, where the 1/n values of Zn^{2+}, Ni^{2+}, and Cd^{2+} were 0.141, 0.137, and 0.099, respectively, less than one which indicates a normal Freundlich isotherm. The adsorption of Zn^{2+}, Ni^{2+}, and Cd^{2+} was reasonably explained by the Langmuir and Freundlich isotherms. However, the Langmuir model yielded the best fit, as the R^2 values were relatively high (close to unity). This is confirmed by the high value of R^2 for Zn^{2+}, Ni^{2+}, and Cd^{2+} in the case of Langmuir which were 0.982, 0.989, and 0.992, respectively, with that of Freundlich, which were 0.947, 0.905, and 0.931, respectively.

Although, the Freundlich isotherm model has lower values of R^2 for Zn^{2+}, Ni^{2+}, and Cd^{2+}, similar trend ($Zn^{2+} > Ni^{2+} > Cd^{2+}$) of Freundlich empirical constants, k and 1/n, were obtained for all metals (see Table 2). Larger values of k mean greater capacities of adsorption [48]. Therefore, sorption capacity and sorption intensity of OSAC for the studied metal ions seem to be $Zn^{2+} > Ni^{2+} > Cd^{2+}$. The results obtained agreed with the works by Shukla and Pai [44] which reported the following order for the sorption of metals onto peat: $Cu^{2+} > Zn^{2+} > Ni^{2+}$. The next, by Shukla and Pai, [44] found a similar order of affinity: $Cu^{2+} > Zn^{2+} > Ni^{2+}$ when investigated with jute fibres. Another, by Iqpal et al. [50], examined petiolar felt-sheath of palm,

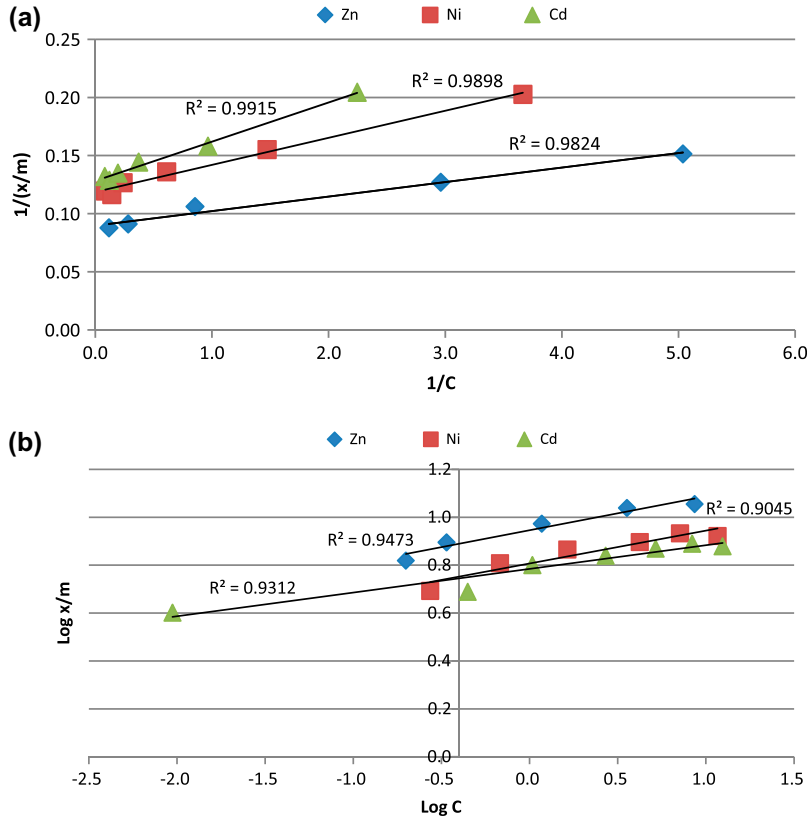

Fig. 7. Langmuir isotherm and Freundlich isotherm for Zn^{2+}, Ni^{2+}, and Cd^{2+} adsorption onto OSAC (contact time, 3 h; shaking speed, 200 rpm; initial pH, 5; initial concentration, 20 mg/L): (a) Langmuir isotherm and (b) Freundlich isotherm.

Table 2
Langmuir and Freundlich isotherm parameters for the adsorption of Zn^{2+}, Ni^{2+} and Cd^{2+} onto OSAC

	Langmuir isotherm model			Freundlich isotherm model		
Parameter	Q (mg/g)	b (L/mg)	i^2	K (mg/g) (L/mg)$^{1/n}$	$1/n$	R^2
Zn	11.14	7.184	0.982	8.83	0.1414	0.947
Ni	8.42	5.094	0.989	6.41	0.1373	0.905
Cd	7.80	3.793	0.992	6.09	0.0989	0.931

and found a slight difference order of affinity: $Pb^{2+} > Cd^{2+} > Cu^{2+} > Zn^{2+} > Ni^{2+}$. Šćiban et al. [51] also reported the following order for wood sawdust: $Cu^{2+} > Zn^{2+} > Cd^{2+}$.

Table 3 lists the comparison of Zn^{2+}, Ni^{2+}, and Cd^{2+} adsorption for various ACs. The results obtained in the present work were comparable with the works reported in the literature. The variation in the Zn^{2+}, Ni^{2+}, and Cd^{2+} adsorption might be due to the different precursors as well as the activation methods and/or conditions used to prepare the ACs.

3.7. Adsorption kinetics

Adsorption kinetics are of great significance to evaluate the performance of a certain adsorbent and gain insight into the underlying mechanisms [52]. Hameed [53] indicates that the kinetic modeling was usually used to investigate the mechanism of adsorption and the potential rate-controlling processes such as mass transfer and chemical reaction. In this study, the modeling of the kinetics of adsorption of Zn^{2+}, Ni^{2+} and Cd^{2+} on OSAC was investigated by two common models, namely, pseudo-first-order model

Table 3
Comparison of the biosorption capacity of different biosorbents

Sorbent	Adsorption capacity (mg/g)			C_0	pH	Ref.
	Zn	Ni	Cd			
Cashew nut shells	–	–	14.29	40	6.0–6.5	[41]
Coir	1.83	2.51	–	74	5.0–6.6	[42]
Oxidised coir	7.88	4.33	–	74	5.0–6.0	[42]
Bagasse fly ash	–	1.12	1.24	12–14	6.0–6.5	[43]
Turkish fly ashes	1.19	0.48	–	25	6.0	[44]
Peanut hull pellets	9	–	6	65	–	[45]
Sphagnum moss peat	–	2.15	–	25	5.0	[46]
Mangosteen shell	–	–	3.15	50	5.0	[32]
Tea waste	–	18.42	–	200	4.0	[47]
Olive stone	–	–	1.85	15	6.0	[48]
Jute fibres	3.55	3.37	–	75	5.5	[33]
Petiolar felt-sheath of palm	6.89	6.0	10.8	100	5.0	[39]
Clinoptilolite (zeolites)	2.7	0.90	3.7	10	4.0–5.0	[49]
Dye loaded groundnut shell	9.57	7.49	–	73	5.0	[33]
Olive stone	11.14	8.42	7.80	20	5.0	This work

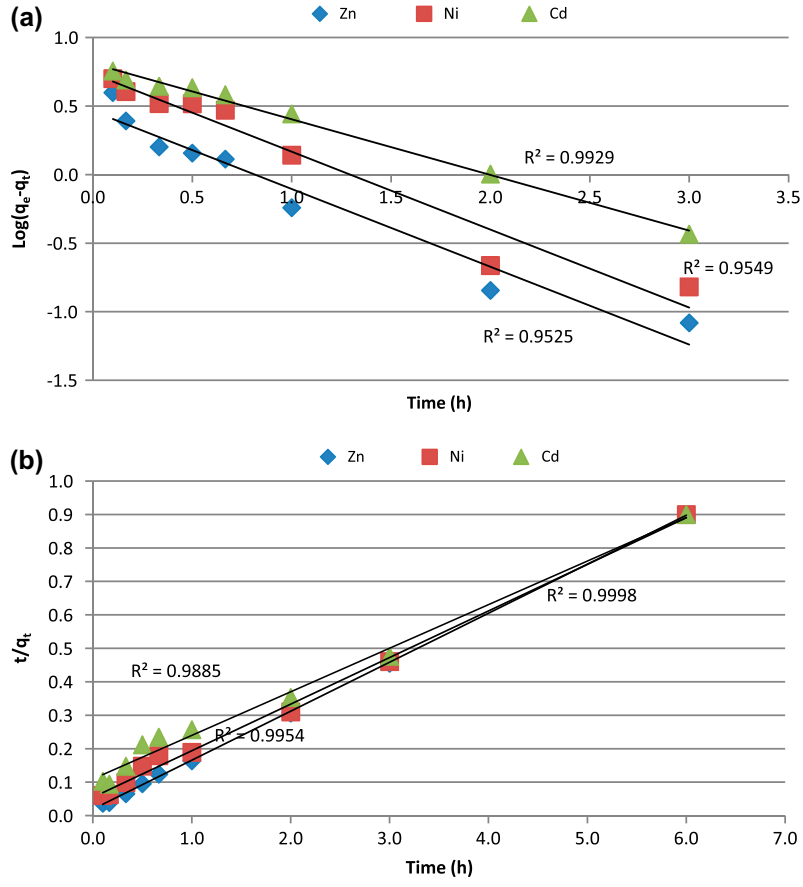

Fig. 8. Kinetic models for Zn^{2+}, Ni^{2+}, and Cd^{2+} adsorption onto OSAC (shaking speed, 200 rpm; initial pH, 5; and initial concentration, 20 mg/L): (a) pseudo-first-order kinetic model, and (b) pseudo-second-order kinetic model.

Table 4
Pseudo-first order and pseudo-second order kinetic model parameters for the adsorption of Zn^{2+}, Ni^{2+} and Cd^{2+} onto OSAC at 20 mg/L concentration

		Pseudo-first order model			Pseudo-second order model		
Parameter	$q_{e,\ exp}$ (mg/g)	K_1 (1/h)	$q_{e,\ cal}$ (mg/g)	R^2	K_2 (g/mg h)	$q_{e,\ cal}$ (mg/g)	R^2
Zn	6.584	1.306	2.903	0.953	1.111	6.831	0.999
Ni	6.515	1.309	5.443	0.955	0.354	7.179	0.995
Cd	6.299	0.935	6.443	0.993	0.155	7.675	0.989

and pseudo-second-order model. The pseudo-first-order model is illustrated as follows [54]:

$$log(q_e - q_t) = log(q_e) - \frac{K_1 t}{2.303} \quad (7)$$

A pseudo-second-order model is described as follows [55]:

$$\frac{t}{q_t} = \frac{1}{k_2 q_e^2} + \frac{t}{q_e} \quad (8)$$

where q_e and q_t (mg/g) are the amounts of adsorbate adsorbed at equilibrium and at any time, t (h), respectively, and k_1 (1/h) is the adsorption rate constant. The linear plot of log $(q_e - q_t)$ vs. t provides a slope of k_1 and intercept of log q_e as shown in Fig. 8(a). The values of k_1 and R^2 obtained from the plots for adsorption of Zn^{2+}, Ni^{2+}, and Cd^{2+} on the adsorbent are reported in Table 4. It was noticed that the R^2 values obtained for the pseudo-first-order model did not show high values. Besides, the experimental q_e values did not agree with the calculated values obtained from the linear plots. This shows that the adsorption of Zn^{2+}, Ni^{2+}, and Cd^{2+} on the adsorbent does not follow a pseudo-first-order kinetic model.

The linear plot of t/q_t vs. t gave $1/q_e$ as the slope and $1/k_2 q_e^2$ as the intercept. Fig. 8(b) shows a good agreement between the experimental and the calculated q_e values. From Table 4, all the R^2 values obtained from the pseudo-second-order model were close to unity, indicating that the adsorption of Zn^{2+}, Ni^{2+}, and Cd^{2+} on OSAC fitted well into this model. A similar result was reported for the adsorption of heavy metals from aqueous solution onto AC from agricultural waste [42].

4. Conclusion

In the present study, the adsorption efficiency of Zn^{2+}, Ni^{2+}, and Cd^{2+} from synthetic wastewater was studied using OSAC. The adsorption of metals was found to increase with increase in OSAC dosage, contact time, and shaking speed. Solution pH > 5 was proved to be more favorable for adsorption of metals on the OSAC. The experimental results showed that 99.03% of Zn^{2+}, 97.34% of Ni^{2+}, and 94.88% of Cd^{2+} were removed at pH 5. Adsorption equilibrium data were fitted to the Langmuir and Freundlich isotherm models and the kinetics data were fitted to the pseudo-second-order kinetics models. The results obtained show that olive stone waste, which has a very low economic value, may be used for the treatment of wastewaters contaminated with heavy metals.

Acknowledgements

The authors wish to acknowledge the Universiti Sains Malaysia (USM) for its financial support under the USM and TWAS Fellowship scheme and RU-PRGS grant scheme (No. 8045048) and acknowledge Ministry of Higher Education, Malaysia for providing LRGS Grant No. (203/PKT/670006) and (03-01-05-SF0502) to conduct this study.

References

[1] P. Verlicchi, A. Galletti, M. Petrovic, D. Barceló, Hospital effluents as a source of emerging pollutants: An overview of micropollutants and sustainable treatment options, J. Hydrol. 389 (2010) 416–428.
[2] M.A. Javed, H.N. Bhatti, M.A. Hanif, R. Nadeem, Kinetic and equilibrium modeling of Pb(II) and Co(II) sorption onto rose waste biomass, Sep. Sci. Technol. 42 (2007) 3641–3656.
[3] T.M. Alslaibi, I. Abustan, Y.K. Mogheir, S. Afifi, Quantification of leachate discharged to groundwater using the water balance method and the Hydrologic Evaluation of Landfill Performance (HELP) model, Waste Manage. Res. 31 (2013) 50–59.
[4] T.M. Alslaibi, Y.K. Mogheir, S. Afifi, Assessment of groundwater quality due to municipal solid waste landfills leachate, J. Environ. Sci. Technol. 4 (2011) 419–436.
[5] T.M. Alslaibi, Y. Mogheir, S. Afifi, Analysis of landfill components in estimating the percolated leachate to groundwater using the HELP model, Water Sci. Technol. 62 (2010) 1727–1734.

[6] T.M. Alslaibi, I. Abustan, M.A. Ahmad, A. Abu Foul, A review: Production of activated carbon from agricultural byproducts via conventional and microwave heating, J. Chem. Technol. Biotechnol. 88 (2013) 1183–1190.
[7] T.M. Alslaibi, I. Abustan, M.A. Ahmad, A. Abu Foul, Review: Comparison of agricultural by-products activated carbon production methods using surface area response, CJASR 2 (2013) 18–27.
[8] A.-N.A. El-Hendawy, A.J. Alexander, R.J. Andrews, G. Forrest, Effects of activation schemes on porous, surface and thermal properties of activated carbons prepared from cotton stalks, J. Anal. Appl. Pyrolysis 82 (2008) 272–278.
[9] N. Yahaya, M. Latiff, I. Abustan, M.A. Ahmad, Effect of preparation conditions of activated carbon prepared from rice husk by $ZnCl_2$ activation for removal of Cu (II) from aqueous solution, Int. J. Eng. Technol. 10 (2010) 27–31.
[10] M. Plaza, C. Pevida, C. Martín, J. Fermoso, J. Pis, F. Rubiera, Developing almond shell-derived activated carbons as CO_2 adsorbents, Sep. Purif. Technol. 71 (2010) 102–106.
[11] R. Boota, H.N. Bhatti, M.A. Hanif, Removal of Cu(II) and Zn(II) using lignocellulosic fiber derived from Citrus reticulata (Kinnow) waste biomass, Sep. Sci. Technol. 44 (2009) 4000–4022.
[12] Q. Cao, K.C. Xie, Y.K. Lv, W.R. Bao, Process effects on activated carbon with large specific surface area from corn cob, Bioresour. Technol. 97 (2006) 110–115.
[13] H.N. Bhatti, M. Amin, Removal of zirconium(IV) from aqueous solution by *Coriolus versicolor*: Equilibrium and thermodynamic study, Ecol. Eng. 51 (2013) 178–180.
[14] S. Erdoğan, Y. Önal, C. Akmil-Başar, S. Bilmez-Erdemoğlu, Ç. Sarıcı-Özdemir, E. Köseoğlu, G. İçduygu, Optimization of nickel adsorption from aqueous solution by using activated carbon prepared from waste apricot by chemical activation, Appl. Surf. Sci. 252 (2005) 1324–1331.
[15] H. Zhang, Y. Yan, L. Yang, Preparation of activated carbon from sawdust by zinc chloride activation, Adsorption 16 (2010) 161–166.
[16] E.S.I. El-Shafey, S.M.Z. Al-Kindy, Removal of $Cu^{2+}$and Ag^{+} from aqueous solution on a chemically-carbonized sorbent from date palm leaflets, Environ. Technol. 34 (2013) 395–406.
[17] A.R. Iftikhar, H.N. Bhatti, M.A. Hanif, R. Nadeem, Kinetic and thermodynamic aspects of Cu(II) and Cr (III) removal from aqueous solutions using rose waste biomass, J. Hazard. Mater. 161 (2009) 941–947.
[18] H.N. Bhatti, R. Khalid, M.A. Hanif, Dynamic biosorption of Zn(II) and Cu(II) using pretreated *Rosa gruss an teplitz* (red rose) distillation sludge, Chem. Eng. J. 148 (2009) 434–443.
[19] A. Hanif, H.N. Bhatti, M.A. Hanif, Removal and recovery of Cu(II) and Zn(II) using immobilized Mentha arvensis distillation waste biomass, Ecol. Eng. 35 (2009) 1427–1434.
[20] C.J. Durán-Valle, M. Gómez-Corzo, V. Gómez-Serrano, J. Pastor-Villegas, M.L. Rojas-Cervantes, Preparation of charcoal from cherry stones, Appl. Surf. Sci. 252 (2006) 5957–5960.
[21] International olive council, World Olive Oil Figures, 2012. Available from: http://www.internationaloliveoil.org/estaticos/view/131-world-olive-oil-figures.
[22] T.M. Alslaibi, I. Abustan, M.A. Ahmad, A. Abu Foul, Application of response surface methodology (RSM) for optimization of Cu^{2+}, Cd^{2+}, Ni^{2+}, Pb^{2+}, Fe^{2+}, and Zn^{2+} removal from aqueous solution using microwaved olive stone activated carbon, J. Chem. Technol. Biotechnol. 88 (2013) 2141–2151.
[23] T.M. Alslaibi, I. Abustan, M.A. Ahmad, A. Abu Foul, Preparation of activated carbon from olive stone waste: Optimization study on the removal of Cu^{2+}, Cd^{2+}, Ni^{2+}, Pb^{2+}, Fe^{2+} and Zn^{2+} from aqueous solution using response surface methodology, J. Dispersion Sci. Technol. (in press), doi: 10.1080/01932691.2013.809506.
[24] T.M. Alslaibi, I. Abustan, M.A. Ahmad, A. Abu Foul, Effect of different olive stone particle size on the yield and surface area of activated carbon production, Adv. Mater. Res. 626 (2013) 126–130.
[25] T.M. Alslaibi, I. Abustan, M.A. Ahmad, A. Abu Foul, Kinetics and equilibrium adsorption of iron (II), lead (II), and copper (II) onto activated carbon prepared from olive stone waste, Desalin. Water Treat. (in press). doi: 10.1080/19443994.2013.833875.
[26] R. Leyva Ramos, L. Bernal Jacome, J. Mendoza Barron, L. Fuentes Rubio, R. Guerrero Coronado, Adsorption of zinc(II) from an aqueous solution onto activated carbon, J. Hazard. Mater. 90 (2002) 27–38.
[27] K. Kadirvelu, K. Thamaraiselvi, C. Namasivayam, Adsorption of nickel(II) from aqueous solution onto activated carbon prepared from coirpith, Sep. Purif. Technol. 24 (2001) 497–505.
[28] K. Kadirvelu, C. Namasivayam, Activated carbon from coconut coirpith as metal adsorbent: Adsorption of Cd(II) from aqueous solution, Adv. Environ. Res. 7 (2003) 471–478.
[29] A. Iup, Manual of symbols and terminology for physico-chemical quantities and units, appendix II, part I, definitions, terminology and symbols in colloid and surface chemistry, Pure Appl. Chem. 31 (1972) 579–638.
[30] M.A. Ahmad, R. Alrozi, Removal of malachite green dye from aqueous solution using rambutan peel-based activated carbon: Equilibrium, kinetic and thermodynamic studies, Chem. Eng. J. 171 (2011) 510–516.
[31] J. Yang, K. Qiu, Preparation of activated carbons from walnut shells via vacuum chemical activation and their application for methylene blue removal, Chem. Eng. J. 165 (2010) 209–217.
[32] N.H. Phan, S. Rio, C. Faur, L. Le Coq, P. Le Cloirec, T.H. Nguyen, Production of fibrous activated carbons from natural cellulose (jute, coconut) fibers for water treatment applications, Carbon 44 (2006) 2569–2577.
[33] A. Ahmad, B. Hameed, Effect of preparation conditions of activated carbon from bamboo waste for real textile wastewater, J. Hazard. Mater. 173 (2010) 487–493.
[34] E.S.Z. El-Ashtoukhy, N. Amin, O. Abdelwahab, Removal of lead (II) and copper (II) from aqueous solution using pomegranate peel as a new adsorbent, Desalination 223 (2008) 162–173.
[35] T.M. Alslaibi, I. Abustan, M.A. Ahmad, A. Abu Foul, Comparison of activated carbon prepared from olive stones by microwave and conventional heating for iron (II), lead (II), and copper (II) removal from

synthetic wastewater, Environ. Prog. Sustainable Energy (in press). doi: 10.1002/ep.11877.
[36] M. Chabani, A. Amrane, A. Bensmaili, Kinetics of nitrates adsorption on Amberlite IRA 400 resin, Desalination 206 (2007) 560–567.
[37] C.F. Baes, R.E. Mesmer, The Hydrolysis of Cations, Wiley, New York, NY, 1976.
[38] S. Ho Lee, C. Hun Jung, H. Chung, M. Yeal Lee, J.W. Yang, Removal of heavy metals from aqueous solution by apple residues, Process Biochem. 33 (1998) 205–211.
[39] T.M. Alslaibi, I. Abustan, M.A. Ahmad, A. Abu Foul, Microwave irradiated and thermally heated olive stone activated carbon for nickel adsorption from synthetic wastewater: A comparative study, AIChE J. 60 (2014) 237–250.
[40] T.M. Alslaibi, I. Abustan, M.A. Ahmad, A. Abu Foul, Cadmium removal from aqueous solution using microwaved olive stone activated carbon, J. Environ. Chem. Eng. 1 (2013) 589–599.
[41] L. Norton, K. Baskaran, T. McKenzie, Biosorption of zinc from aqueous solutions using biosolids, Adv. Environ. Res. 8 (2004) 629–635.
[42] A.B. Pérez-Marín, V.M. Zapata, J.F. Ortuño, M. Aguilar, J. Sáez, M. Lloréns, Removal of cadmium from aqueous solutions by adsorption onto orange waste, J. Hazard. Mater. 139 (2007) 122–131.
[43] R. Zein, R. Suhaili, F. Earnestly, E. Indrawati, Removal of Pb(II), Cd(II) and Co(II) from aqueous solution using Garcinia mangostana L. fruit shell, J. Hazard. Mater. 181 (2010) 52–56.
[44] S. Shukla, R.S. Pai, Adsorption of Cu(II), Ni(II) and Zn (II) on modified jute fibres, Bioresour. Technol. 96 (2005) 1430–1438.
[45] I. Langmuir, The adsorption of gases on plane surfaces of glass, mica and platinum, J. Am. Chem. Soc. 40 (1918) 1361–1403.
[46] U. Saha, S. Taniguchi, K. Sakurai, Simultaneous adsorption of cadmium, zinc, and lead on hydroxyaluminum- and hydroxyaluminosilicate-montmorillonite complexes, Soil Sci. Soc. Am. J. 66 (2002) 117–128.
[47] T.W. Webi, R.K. Chakravort, Pore and solid diffusion models for fixed-bed adsorbers, AIChE J. 20 (1974) 228–238.
[48] H.A. Aziz, M.S. Yusoff, M.N. Adlan, N.H. Adnan, S. Alias, Physico-chemical removal of iron from semi-aerobic landfill leachate by limestone filter, Waste Manage. 24 (2004) 353–358.
[49] I. Tan, A. Ahmad, B. Hameed, Optimization of preparation conditions for activated carbons from coconut husk using response surface methodology, Chem. Eng. J. 137 (2008) 462–470.
[50] M. Iqbal, A. Saeed, N. Akhtar, Petiolar felt-sheath of palm: A new biosorbent for the removal of heavy metals from contaminated water, Bioresour. Technol. 81 (2002) 151–153.
[51] M. Šćiban, B. Radetić, Ž. Kevrešan, M. Klašnja, Adsorption of heavy metals from electroplating wastewater by wood sawdust, Bioresour. Technol. 98 (2007) 402–409.
[52] H. Qiu, L. Lv, B. Pan, Q. Zhang, W. Zhang, Critical review in adsorption kinetic models, J. Zhejiang Univ. Sci. A 10 (2009) 716–724.
[53] B. Hameed, Spent tea leaves: A new non-conventional and low-cost adsorbent for removal of basic dye from aqueous solutions, J. Hazard. Mater. 161 (2009) 753–759.
[54] Y. Ho, G. McKay, Sorption of dye from aqueous solution by peat, Chem. Eng. J. 70 (1998) 115–124.
[55] Y. Ho, G. McKay, Pseudo-second order model for sorption processes, Process Biochem. 34 (1999) 451–465.